https://doi.org/10.5194/esurf-2022-72
Preprint. Discussion started: 23 January 2023

Earth Surface Dynamics Discussions
Open Access
EGU

On the use of packing models for the prediction of fluvial sediment porosity

Christoph Rettinger[1,2], Mina Tabesh[1,3], Ulrich Rüde[2,4], Stefan Vollmer[1], and Roy M. Frings[5]

[1]Department of Fluvial Morphology, Sediment Dynamics and Management, Federal Institute of Hydrology, Am Mainzer Tor 1, Koblenz, 56068,Germany
[2]Chair for System Simulation, Friedrich-Alexander-Universität Erlangen-Nürnberg, Cauerstraße 11, Erlangen, 91052, Germany
[3]Institute of Hydraulic Engineering and Water Resources Management, RWTH Aachen University,Mies-van-der-Rohe-Straße 17, Aachen, 52074, Germany
[4]CERFACS, 42 Avenue Gaspard Coriolis, Toulouse Cedex 1, 31057, France
[5]Rijkswaterstaat Zuid-Nederland, Ministry of Infrastructure and Water Management, Avenue Ceramique 125, Maastricht, 6221 KV, The Netherlands

Correspondence: Christoph Rettinger (christoph.rettinger@fau.de)

Abstract. Obtaining accurate porosity information of fluvial sediment deposits is helpful and desirable for many tasks of river engineers. Besides direct measurements of single samples and empirical formulas specialized for specific cases, packing models promise efficient predictions due to their theoretical and extensible foundation. The objective of this work is thus to investigate the usability of three such models in order to obtain a suitable porosity prediction method for the challenging case of fluvial sediment packings. There, the complexity originates from wide continuous size distributions, from silt to gravel, and different grain shapes. We use data obtained from extensive numerical packing simulations to determine the required model parameters and to verify the models' accuracy for moderate size ratios. This study reveals systematic deficits in one of the models which can be attributed to the absence of a built-in mixture packing model. By combining these findings with data from laboratory measurements and extending the model to include cohesive effects, we exemplify for the Rhine River in Germany that reasonable porosity predictions can be obtained with the Compressible Packing Model. Through an additional comparison with data from French rivers, guidelines for a successful prediction in cases with limited prior knowledge of the model parameters are developed. Future model enhancements, of the packing models directly as well as by incorporating more effects that are known to influence porosity, are expected to improve the predictive performance.

1 Introduction

Porosity is one of the key structural properties of fluvial sediment deposits as it links bed level changes to the amount of transported material (Coleman and Nikora, 2009), affects the permeability and mobility of the river bed (Fraser, 1935; El-Husseiny, 2020; Rettinger et al., 2022a), and determines the quality of habitats for aquatic organisms (Noack et al., 2017). River-related research thus requires its accurate and efficient assessment where it is known to vary along a river's length and width (Frings et al., 2011; Tabesh et al., 2022). This variation originates from spatial changes in factors that influence porosity,

https://doi.org/10.5194/esurf-2022-72
Preprint. Discussion started: 23 January 2023


Earth Surface Dynamics Discussions
Open Access
EGU

often quite significantly (Fraser, 1935; Frings et al., 2011). Examples for such factors are the sediment grain size distribution (Frings et al., 2011; Tabesh et al., 2022), the grain form and shape (Cho et al., 2006; Chang et al., 2018; Zhang et al., 2020; Rettinger et al., 2022b), the deposition conditions leading to loose or dense packings (An et al., 2008; Chang et al., 2018), and the type of micromechanical grain interaction like friction and cohesive forces (Yu et al., 2003; An et al., 2008; Zou et al., 2011; Liu et al., 2017; Zhang et al., 2020).

Porosity of sediment packings can be determined in various ways where all come with individual benefits and challenges. The straightforward way is to carry out field studies or laboratory measurements, for which different techniques have been developed (Frings et al., 2011; Seitz et al., 2018; Tabesh et al., 2019). While field studies are extremely laborious and might suffer from measurement uncertainties, laboratory studies might additionally influence porosity by the confined setting and the packing process (Zou and Yu, 1995). Using numerical simulations of the packing process is a more recent approach and offers the advantage to have full control over all parameters (Liang et al., 2015; Schruff et al., 2018; Seelen et al., 2018; Zhang et al., 2020), allowing for systematic studies of the different porosity controlling factors (Suhr and Six, 2020; Rettinger et al., 2022b). All these techniques have in common that they provide direct measurements of porosity for specific cases, making them a valuable source for porosity data sets. However, they are generally too costly to be applied for a multitude of porosity assessments and require the actual sediment grains for field or laboratory studies, or precise knowledge about their properties to be used in numerical simulations.

On the other hand, empirical porosity predictors have been developed as an effective alternative. They commonly rely on statistical descriptors of the grain properties, like the mean grain size (Carling and Reader, 1982; Wu and Wang, 2006), its standard deviation (Wooster et al., 2008), or the percentage of fine particles (Frings et al., 2011). These predictors are typically given by a concise mathematical formula and, by construction, require only very limited information about the packing, making them easily applicable. However, as they were obtained through fitting to a specific data set, their accuracy for other cases is low (Frings et al., 2011) and there is no systematic way to extend them to other porosity-modifying factors. Thus, a more theoretical, model-based description of packing properties and their effect on porosity is desirable in order to obtain a generally applicable and extensible predictor.

Such a framework is offered by so-called packing, or mixture, models. Pioneered by Furnas (1931) and Westman (1936), the general idea of these models is to regard the system as consisting of a finite number of separate particle classes with different properties. Then, the pair-wise interaction among these classes and their effect on porosity is modeled and, finally, adequately combined to obtain an estimation of the system's porosity. While some of these models have been applied to packings of distinct particle shapes, like sphere-cylinder systems (Yu et al., 1996), the majority focuses on the grain size to distinguish the classes (Jones et al., 2002; Kwan et al., 2013; Liu et al., 2020). Most of them have been developed in the context of industrial and engineering applications where usually only a small number of well-defined and well-separated size classes are mixed together, resulting in a large number of models for binary (Kamann et al., 2007; Zhang et al., 2011; Chang and Deng, 2017; Roquier, 2017; Wu and Li, 2017) and ternary packings (Kwan et al., 2015; Perera et al., 2022). Commonly, they consider the filling effect, meaning that fine particles fill the pores between the tightly packed coarse particles, and the occupation effect, meaning that some coarse particles completely occupy the space in place of tightly packed fine particles, see Fig. 1. In both

https://doi.org/10.5194/esurf-2022-72
Preprint. Discussion started: 23 January 2023

Earth Surface Dynamics Discussions
Open Access
EGU

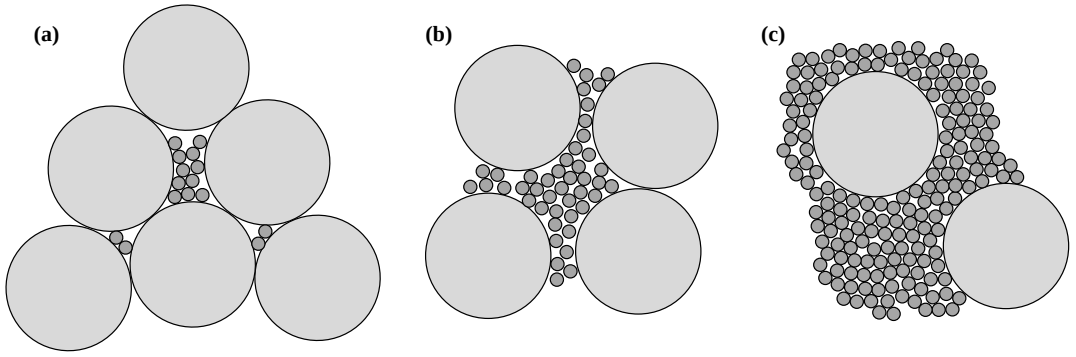

Figure 1. Packing configurations considered and modeled by packing models. **a** filling, **b** interacting, **c** occupation.

cases, the main component of the packing, i.e., coarse for filling and fine for occupation, is essentially left unchanged, and the presence of the second component decreases porosity. For cases between these two limits, however, there is a mutual interaction between the different components of the packing (Fig. 1b). There, the models differ in the type of these interactions that are included and how these are modeled, where typically each additional effect introduces new model parameters (Kwan et al., 2013). In comparative studies for binary mixtures of quartz sand (Liu et al., 2020) and ternary mixtures of cement (Jones et al., 2002), the general applicability of these models has been demonstrated, with minor differences in specific cases.

Turning towards packings of fluvial sediment, an immediate challenge arises due to the large grain size range, covering silt, sand, and gravel, which leads to a wide range of size ratios on the order of 10^4 between the largest and the smallest grains. The observable grain sizes naturally cover the whole range of this size interval, in stark contrast to strictly binary or ternary packings for which these packing models have been primarily designed and used. Only a small subset of the above mentioned packing models was developed for such multi-sized cases (Yu and Standish, 1991; De Larrard, 1999; Chang and Deng, 2018; Liu et al., 2019) and their verification was often again restricted to a few different size classes. Additionally, size-dependent effects like cohesive interactions become relevant once small particles like fine sand and silt are involved which again influence the packing (Yu et al., 2003; Zou et al., 2011). Furthermore, the average grain shape varies from river to river (Oakey et al., 2005; Liang et al., 2015; Rettinger et al., 2022b), in contrast to the usually rather similar and often simpler shapes encountered in industrial applications. The shape is known to strongly influence the interaction among grains which must be accounted for in the model (Yu et al., 1996). Frings et al. (2011) could demonstrate that the model proposed by Yu and Standish (1991) is generally able to produce reasonable predictions of porosity for fluvial packings, but the model parameters and their influence on the results remained difficult to determine. All in all, the applicability and accuracy of such packing models, their adequate parameterization, and a guideline on which one to use for porosity predictions of fluvial sediment deposits is currently missing.

The main objective of the present manuscript is thus to fill this apparent gap by providing a systematic and comparative study of multi-sized packing models in order to derive a suitable porosity predictor. The models are parameterized with data from laboratory experiments and numerical simulations with fluvial sediment, and subsequently verified for different grain size distributions. In line with this idea, the paper is structured as follows: Section 2 reviews different packing models proposed in

https://doi.org/10.5194/esurf-2022-72
Preprint. Discussion started: 23 January 2023


Earth Surface Dynamics Discussions
Open Access
EGU

literature for the packing of a large number of size classes. Then, the models' interaction parameters are calibrated in Sect. 3 with the help of numerical simulations of binary packings. In Sect. 4, these models are validated for sand-gravel mixtures that were again obtained from numerical simulations to check their extension to multi-sized packings. Section 5 further extends the validation to the full size range of fluvial sediment contained in laboratory measurements, necessitating a model extension for cohesion, and discusses the applicability to sediment data from two different rivers. Section 6 summarizes the main findings and outlines future directions.

2 Review of Packing Models

This section presents several packing models that have been proposed for multi-size packings. For all of them, we provide a concise but complete summary, followed by a direct comparison of the models.

2.1 Definitions

Depending on the scientific community, the packing of solids is commonly described by different quantities like porosity, the solid packing fraction, the void ratio, or the specific volume. As a consequence, the available packing models are formulated differently. However, all of them can be directly converted to provide an estimate for porosity, which is the focus of this work.

Considering a system of total volume V, that contains solid particles of volume V_s and pore (or void) volume V_p such that $V = V_s + V_p$, then the quantities mentioned above are given as:

porosity
$$n = \frac{V_p}{V} \in [0,1] \tag{1}$$

solid packing fraction (or density)
$$\phi = \frac{V_s}{V} = 1 - n \in [0,1] \tag{2}$$

void ratio (or voids index)
$$e = \frac{V_p}{V_s} = \frac{n}{1-n} \in [0,\infty) \tag{3}$$

specific volume
$$\nu = \frac{V}{V_s} = \frac{1}{1-n} \in [1,\infty) \tag{4}$$

Generally, the solid volume contains particles of various sizes and shapes as commonly encountered in fluvial sediment deposits. Analogously to sieving the particles with a hierarchy of sieves of mesh sizes s_i, we assume that the particles can be partitioned into N classes based on their size. The average class size d_i is calculated as the geometric mean of the respective sieve interval $[s_i\, s_{i+1}]$, i.e.,

$$d_i = \sqrt{s_i\, s_{i+1}}. \tag{5}$$

This measure, like the sieving procedure, corresponds to a discretization of the continuous grain size distribution and is necessary as the here considered packing models can only cope with discrete classes of a given size. The N size classes are ordered such that $d_1 > d_2 > \cdots > d_N$. The size ratio of two size classes is defined as

$$r_{ij} = \begin{cases} d_i/d_j, & d_i \le d_j, \\ d_j/d_i, & d_i > d_j, \end{cases} \tag{6}$$

https://doi.org/10.5194/esurf-2022-72
Preprint. Discussion started: 23 January 2023

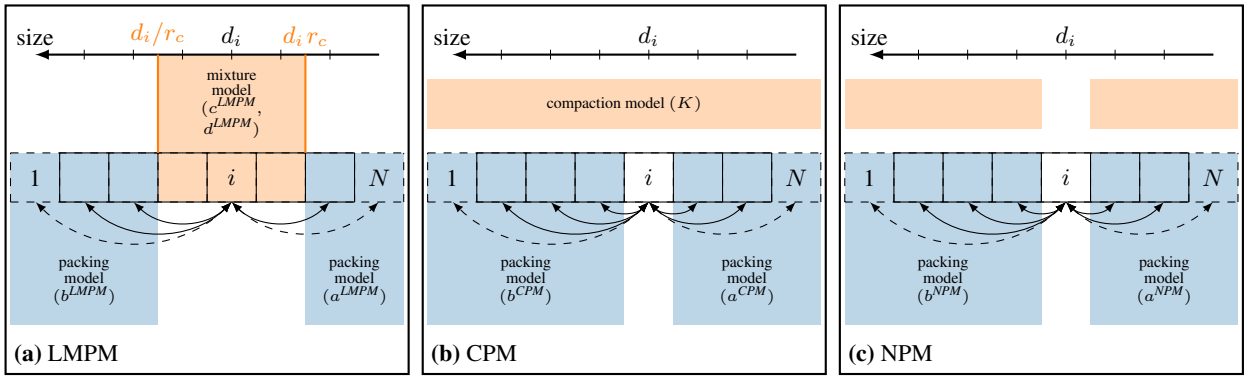

Figure 2. Graphical representation of the packing models considered in this study, Sects. 2.2 to 2.4, and their modeled interactions among the discrete size classes 1 to N (depicted as boxes) via the given interaction functions. Blue shading indicates pair-wise interaction while orange shading implies multi-component interaction among the contained size classes.

such that $r_{ij} \in [0,1]$ and $r_{ij} = r_{ji}$. The subscripts i, j, and later on also k, are used to denote quantities of distinct size classes.

The partial volume fraction of size class i is obtained as

$$y_i = \frac{V_{s,i}}{V_s}, \tag{7}$$

such that $\sum_{i=1}^{N} y_i = 1$. Since we assume a constant material density for all particles, the y_i correspond to the mass fractions obtained by the sieving procedure. Additionally, we further assume a known initial porosity $n_{0,i}$ which would be observed for a system containing only particles of size class i, i.e., a uniform packing.

These quantities $(d_i, y_i, n_{0,i})$ are the input for all packing models considered here. Those are presented next and we stick mostly to the original formulation and notation, with slight adaptions for clarity and consistency. While an in-depth discussion of the derivation and specifics of each model are out of scope and can be found in the original work, we state the resulting model and mention the underlying assumptions. Generally, the idea of such packing models is to assume that one or several size classes form the dominant component, and the others are either fillers or embedded into this dominant size class. Differences between the models mainly originate from the way which and how the porosity-modifying effects of these other size classes are mathematically modeled. Since it is not known a-priori which of the N size classes is the dominant one, all possibilities are considered and the one yielding the densest packing is taken.

For all models, the simplified binary versions are stated in Appendix B. Additionally, we provide a Python implementation together with exemplary cases in the supplementary material.

2.2 Linear Mixture Packing Model

The Linear Mixture Packing Model (LMPM) was originally proposed by Yu and Standish (1991) and combines a linear packing model (LPM) with a mixture packing model (MM). Later, the packing model was slightly modified by Yu et al. (1996) to account for different initial porosities of the individual classes, as e.g. encountered for deposits with differently

https://doi.org/10.5194/esurf-2022-72
Preprint. Discussion started: 23 January 2023

shaped particles. We here present the modified variant, which also simplified some of the involved parameters. The model is formulated in terms of the specific volume, where ν_i denotes the one of a uniform packing of a single size class, i.e.,

$$\nu_i = \frac{1}{1 - n_{0,i}}. \tag{8}$$

Considering the size class i, the general idea is to separate all size classes into three categories, depending on their relative sizes. Then, the partial specific volume can be obtained as

$$\nu_i^* = \sum_{j=1}^{L-1} (\nu_j - (\nu_j - 1) b^{LMPM}(r_{ij})) y_j + \nu_i^{mix} \sum_{j=L}^{M} y_j + \sum_{j=M+1}^{N} \nu_j (1 - a^{LMPM}(r_{ij})) y_j, \tag{9}$$

with the interaction functions a^{LMPM} (Eq. (A3)) and b^{LMPM} (Eq. (A4)). The second term represents the controlling component, containing not only the class i but all classes $[L, M]$, which interact according to the mixture packing model

$$\nu_i^{mix} = \nu_0^{mix} + \frac{\sum_{j=L}^{M-1} \sum_{k=j+1}^{M} c^{LMPM}(r_{jk}, n_{0,mix}) y_j y_k}{\left(\sum_{j=L}^{M} y_j\right)^2} + \frac{\sum_{j=L}^{M-1} \sum_{k=j+1}^{M} d^{LMPM}(r_{jk}, n_{0,mix}) y_j y_k (y_j - y_k)}{\left(\sum_{j=L}^{M} y_j\right)^3} \tag{10}$$

where $\nu_0^{mix} = \frac{\sum_{j=L}^{M} y_j \nu_j}{\sum_{j=L}^{M} y_j}$, and c^{LMPM} and d^{LMPM} are the quadratic and cubic mixture parameters, respectively, as given by Eqs. (A5) and (A6). Thus, in total, the model requires four parameters.

By introducing the critical size ratio of entrance r_c, the classes L and M are the minimum and maximum ones whose sizes are between d_i / r_c and $d_i \, r_c$, see Eq. (A1) and Eq. (A2). If $L = M = i$, the LMPM reduces to the linear packing model Yu et al. (1996) whereas the mixture model is recovered for $L = 1$ and $M = N$. Based on geometric arguments for tetrahedral sphere packings, $r_c = 0.154$ was suggested (Yu and Standish, 1991). A graphical representation of the model is given in Fig. 2 a.

Finally, the specific volume of the packing is obtained as

$$v = \max_i \nu_i^*. \tag{11}$$

By introducing more parameters, the linear packing model has recently been extended to take into account additional interaction mechanisms, like the wedging effect (Kwan et al., 2013, 2015), however, only for binary and ternary packings. Furthermore, the combination with a mixture model has recently been revised (Chang and Deng, 2017, 2018) which led to a system of nonlinear equations that needs to be solved. For simplicity, we will here make use of the above presented model.

2.3 Compressible Packing Model

The Compressible Packing Model (CPM) was presented by De Larrard (1999) in the context of concrete mixing. It is a three-parameter model that is formulated in terms of particle packing densities and first constructs an ideal packing with maximal packing density. Then, the effect of the imperfect packing process is considered by a compaction index which determines the actual packing density of the deposit.

https://doi.org/10.5194/esurf-2022-72
Preprint. Discussion started: 23 January 2023


Earth Surface Dynamics Discussions
Open Access
EGU

The ideal case is obtained by using a linear packing model, similar to the LPM above, assuming a single dominant size class i, for which the solid packing fraction is obtained as:

$$\gamma_i = \frac{\beta_i}{1 - \sum_{j=1}^{i-1} \left(1 - \beta_i + b^{CPM}(r_{ij})\,\beta_i(1 - \frac{1}{\beta_j})\right) y_j - \sum_{j=i+1}^{N} \left(1 - a^{CPM}(r_{ij})\,\frac{\beta_i}{\beta_j}\right) y_j}, \tag{12}$$

where β_i and β_j are the so-called ideal, i.e., maximum, packing densities of classes i and j, respectively, and a^{CPM} and b^{CPM} are the model's interaction functions, see Eqs. (A7) and (A8).

The ideal packing density of the complete packing would then be obtained as

$$\gamma = \min_i \gamma_i. \tag{13}$$

The actual packing density ϕ is implicitly obtained as the solution of

$$K = \sum_{i=1}^{N} \frac{y_i/\beta_i}{1/\phi - 1/\gamma_i}. \tag{14}$$

The compaction index $K \in (0, \infty)$ models the packing process and state, since actual packings are generally not ideal and exhibit less densely packed configurations. In the literature, suggested values for K from 4 for a loose packing (De Larrard, 1999) to 12.5 for a compressed one (Jones et al., 2002) can be found, while $K \to \infty$ would recover the ideal packing density γ. By construction, there is only a single ϕ that satisfies this equation in the range $\phi \in (0, \gamma)$ which we here determine via a bisection line search after reformulation into a root-finding problem. Figure 2 b visualizes this model.

To be consistent with our notion of $n_{0,i}$, which is the actually observed porosity for a uniform packing, we apply Eq. (14) for a single size class and obtain

$$\beta_i = \frac{K+1}{K}(1 - n_{0,i}). \tag{15}$$

The CPM has been extended based on geometrical considerations for the loosening effect by an additional parameter (Roquier, 2017), however, again only for binary packings. Therefore, we will apply the original CPM.

2.4 Nonlinear Packing Model

Recently, Liu et al. (2019) developed the Nonlinear Packing Model (NPM) in order to improve upon deficits of the linear packing model for binary mixtures. It is formulated based on void ratios, where ϵ_i is the void ratio of a single size class i, i.e.,

$$\epsilon_i = \frac{n_{0,i}}{1 - n_{0,i}}. \tag{16}$$

Assuming i to be the single dominant component, the corresponding void ratio is then modeled as[1]:

$$\epsilon_i^* = \epsilon_i y_i^2 - \sum_{\substack{j=1 \\ j \neq i}}^{N} \left(\epsilon_j y_j^2 - 2\epsilon_j y_j + \sum_{\substack{k=j+1 \\ k \neq i}}^{N} (\epsilon_j + \epsilon_k) y_j y_k \right) - \sum_{j=1}^{i-1} b^{NPM}(r_{ij})\,\epsilon_j (1+y_i) y_j - \sum_{j=i+1}^{N} a^{NPM}(r_{ij})\,(\epsilon_j (1+y_i) + 1) y_j. \tag{17}$$

[1]We corrected a mistake in the original work in Eq. 18 (Liu et al., 2019) in the fourth term with $\sum_{\substack{k=1 \\ k \neq i,j}}^{n}$, as can be verified by checking against the results for the ternary packings in Eqs. 13-15.

https://doi.org/10.5194/esurf-2022-72
Preprint. Discussion started: 23 January 2023

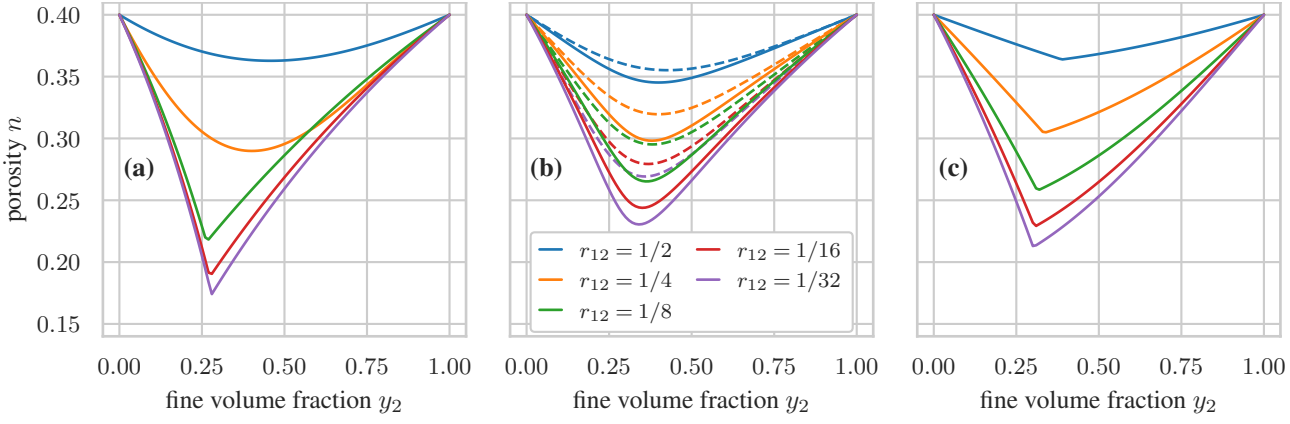

Figure 3. Comparison of the three different packing models for binary cases with $n_{0,1} = n_{0,2} = 0.4$. **a** LMPM, **b** CPM, with $K = 4$ (dashed) and $K = 9$ (solid), **c** NPM.

The two interaction functions a^{NPM} and b^{NPM} are given in Eqs. (A9) and (A10).

The void ratio of the packing is then obtained as

$$e = \max_i \epsilon_i^*. \tag{18}$$

The model is sketched in Fig. 2 c.

2.5 Comparison

While an in-depth comparison of the models and their performance for the specific case of fluvial sediment will be given in the upcoming sections, it is worthwhile to compare them more generally for the parameterization commonly applied in literature. A direct comparison in terms of predicted porosity for binary packings with varying volume fractions and size ratios is shown in Fig. 3, using the parameterization as stated in Appendix A. For the two extreme cases, $y_2 = 0$ and $y_2 = 1$, where only a single size class is present in the packing, all models yield the same porosity, as imposed through $n_{0,1} = n_{0,2} = 0.4$. In between, the differences of the three models are directly visible, in the general shape of the curves as well as the obtained porosity values. Considering a single model, the different predictions for changing size ratios originate solely from the fact that the interaction parameters are modified as a function of the size ratio. Specifically, for the LMPM, the switching between the two intrinsic models, packing and mixing, is apparent in the distinct shape of the curve once the size ratio is below 0.154, the value of r_c. For the CPM, the influence of the compaction index K can be seen where for larger values smaller porosity values are obtained.

Apart from the general model itself, the differences originate from the applied interaction functions. All models feature parameters a and b that were introduced to express similar interactions between the size classes as a function of r_{ij}. However, those interaction functions should usually be seen in the context of the model itself and thus take different forms and values, which does not permit a comparative interpretation whether or not certain interactions are taken into account. These interaction functions are shown in Fig. 4. While the functions for the LMPM and the NPM reach their maximum for the case $r_{ij} \to 0$

https://doi.org/10.5194/esurf-2022-72
Preprint. Discussion started: 23 January 2023

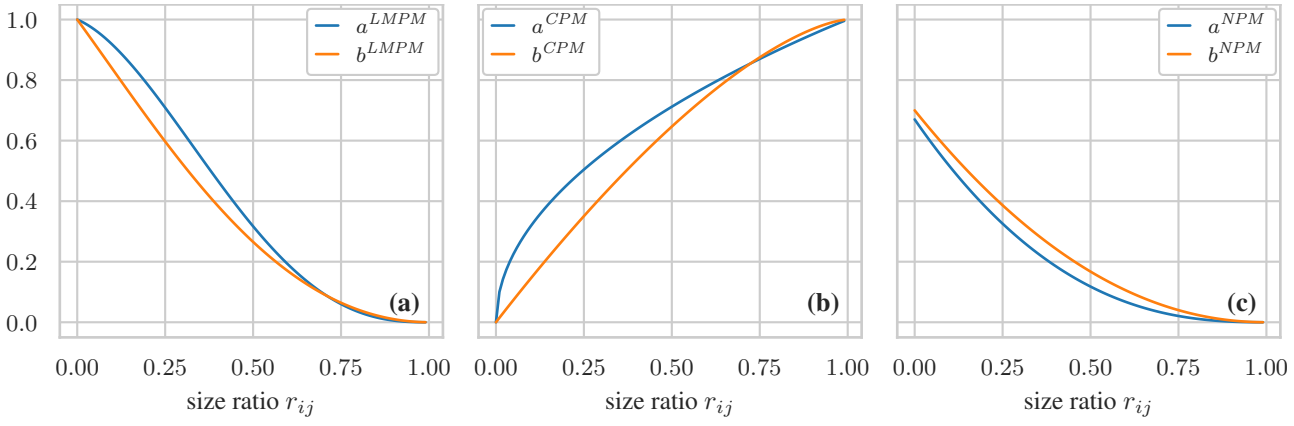

Figure 4. Comparison of interaction functions proposed in literature for spherical particles for the three different packing models. **a** LMPM, **b** CPM, **c** NPM.

and are 0 for $r_{ij} = 1$, it is the other way around for the CPM. Due to the introduction of additional prefactors in Eqs. (A9) and (A10), the maximum of the NPM is below 1 while this is the explicitly enforced value in the LMPM and CPM. Still, there is a general similarity between the models which have inspired different modifications of the functional form of these interaction parameters (Kwan et al., 2013; Chan and Kwan, 2014; Knop and Peled, 2016; Chang and Deng, 2017; Roquier, 2017). Furthermore, as noticed by several authors, the interaction functions usually depend on the shape of the particles (Kwan et al., 2013; Liu et al., 2019). Consequently, the functions' coefficients have to be calibrated for a specific case in order to yield accurate predictions of the packing porosity. This calibration is carried out next for our specific case of fluvial sediment.

3 Calibration of interaction parameters

In this section, binary packings of sedimentary particles were simulated and their porosity was evaluated in order to obtain the interaction parameters required for the packing models presented in Sect. 2.

3.1 Simulation setup

For this study, we made use of the numerical method, the simulation setup and the evaluation approach that had been validated extensively in a similar recent study by Rettinger et al. (2022b) and were contained in the WALBERLA simulation framework (Bauer et al., 2021). Here, for brevity, we just summarize the key aspects and specifics of the simulation setup and refer to the original work for an in-depth discussion of all parts.

The packings were simulated in a horizontally periodic domain of size 0.25 m $\times$0.25 m, by generating and dropping 25 kg of particles onto the bottom plane. All particles had a density of $\rho_p = 2650\,\mathrm{kg/m^3}$. For each grain, the size was chosen from the complete interval of the sieve mesh size corresponding to the respective size class, assuming a uniform distribution within this interval. Following the previous findings (Rettinger et al., 2022b), we also assumed that the shape of all particles

https://doi.org/10.5194/esurf-2022-72
Preprint. Discussion started: 23 January 2023

Earth Surface Dynamics Discussions
Open Access
EGU

Table 1. Sieve mesh sizes and correspondingly considered mean sizes d_i.

sieve mesh sizes (mm)	22.4 - 31.5	16 - 22.4	11.2 - 16	8 - 11.2	5.6 - 8	4 - 5.6	2.8 - 4
d_i (mm)	26.56	18.93	13.39	9.47	6.69	4.73	3.35

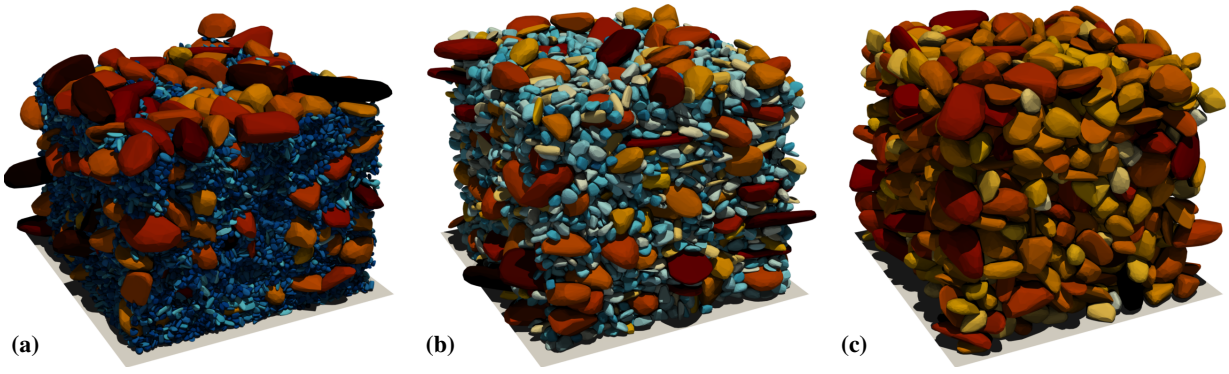

Figure 5. Visualization of three different binary packings for the case $y_1 = y_2 = 0.5$ with $d_1 = 26.56$ mm and (a) $d_2 = 4.73$ mm with 49 788 particles, (b) $d_2 = 9.47$ mm with 7 625 particles, (c) $d_2 = 18.93$ mm with 1190 particles. Color depicts the size on a logarithmic scale.

is similar and independent of the actual size, such that there are no shape-differences between size classes. Thus, each particle shape was randomly sampled from a set of meshes (Rettinger et al., 2022c), obtained by computer tomography (CT) scans of actual gravel-sized sediment from the Rhine River in Germany with an average flatness of 0.647 and average elongation of 0.682. During the generation phase of the simulation and continued for 12 s, we applied a slight horizontal shaking of the whole domain to consolidate the packing. Afterward, a force-based damping, similar to Zhao et al. (2017), was applied until all particles had come to rest. Porosity was determined from the bulk region of the resulting packing, thus excluding possible finite size effects due to the bottom wall and top surface. This evaluation was achieved by first assessing the horizontally averaged porosity profile as a function of packing height based on the available grain positions and their size information, and then computing the average of this profile over the height interval of the bulk region.

The binary packings were here generated for particles with sizes between 2.8 mm and 31.5 mm. The extent of the size classes and their mean sizes according to Eq. (5) are given in Table 1. The packings were composed of a mixture of the coarse size class and one of the others, which varies the size ratio, and applying nominal mass fractions $y_1 \in \{0, 0.1, \ldots, 0.9, 1\}$ and $y_2 = 1 - y_1$. Due to the random sampling in the generation routine, the actually generated mass fractions might vary. Three examples are visualized in Fig. 5. Each of these simulations was typically run on 100 - 1824 compute cores for several hours, depending on the number of particles.

https://doi.org/10.5194/esurf-2022-72
Preprint. Discussion started: 23 January 2023

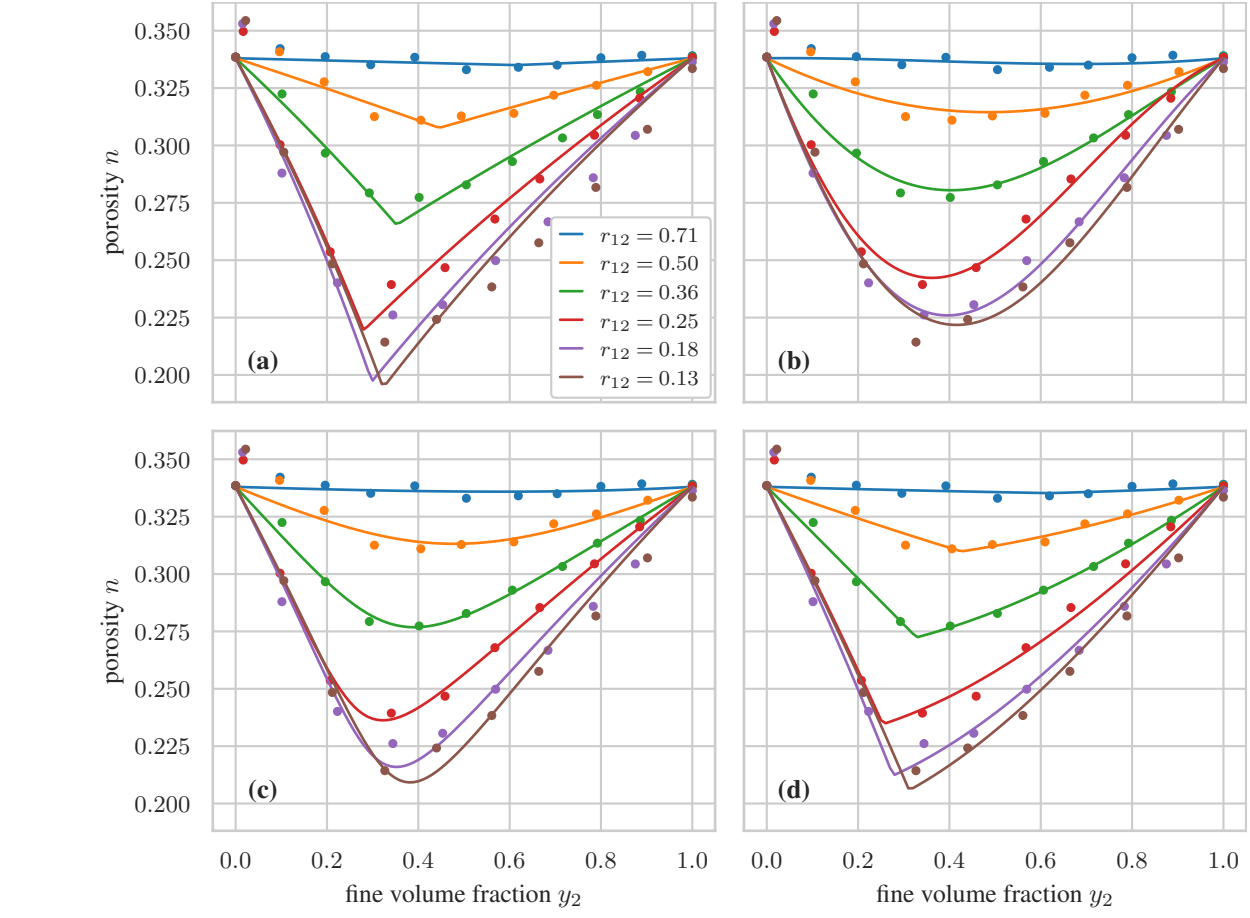

Figure 6. Comparison of the different prediction models for the simulated binary setups with Rhine sediment. **a** LPM ($R^2 = 0.95$, RMSE $= 0.008$), **b** MM ($R^2 = 0.97$, RMSE $= 0.007$), **c** CPM ($R^2 = 0.97$, RMSE $= 0.006$), **d** NPM ($R^2 = 0.98$, RMSE $= 0.006$).

3.2 Evaluation

For gravel-sized sediment with non-cohesive interactions, the actual grain size of uniform packings should not influence porosity (Frings et al., 2011). Thus, the initial porosity values $n_{0,i}$ were assumed to be constant for all size classes and taken as the average of the porosity values for the uniform cases from the simulations. Here, this resulted in $n_{0,i} = 0.338 \pm 0.002$ for all size classes i. This value is slightly less than the typically used value of 0.36 for random sphere packings, which can be attributed to the non-spherical sediment shape (Rettinger et al., 2022b).

Then, for each of the combinations of two different size classes, the binary variants of the packing models as given in Appendix B were directly fit to the resulting curves as a function of the mass fraction in order to determine the two free parameters. Here, we consider the two components of the LMPM, LPM and MM, separately as they are essentially two distinct models with separate model parameters. For the CPM, the only three-parameter model, a compaction index of $K = 9$ was used

https://doi.org/10.5194/esurf-2022-72
Preprint. Discussion started: 23 January 2023

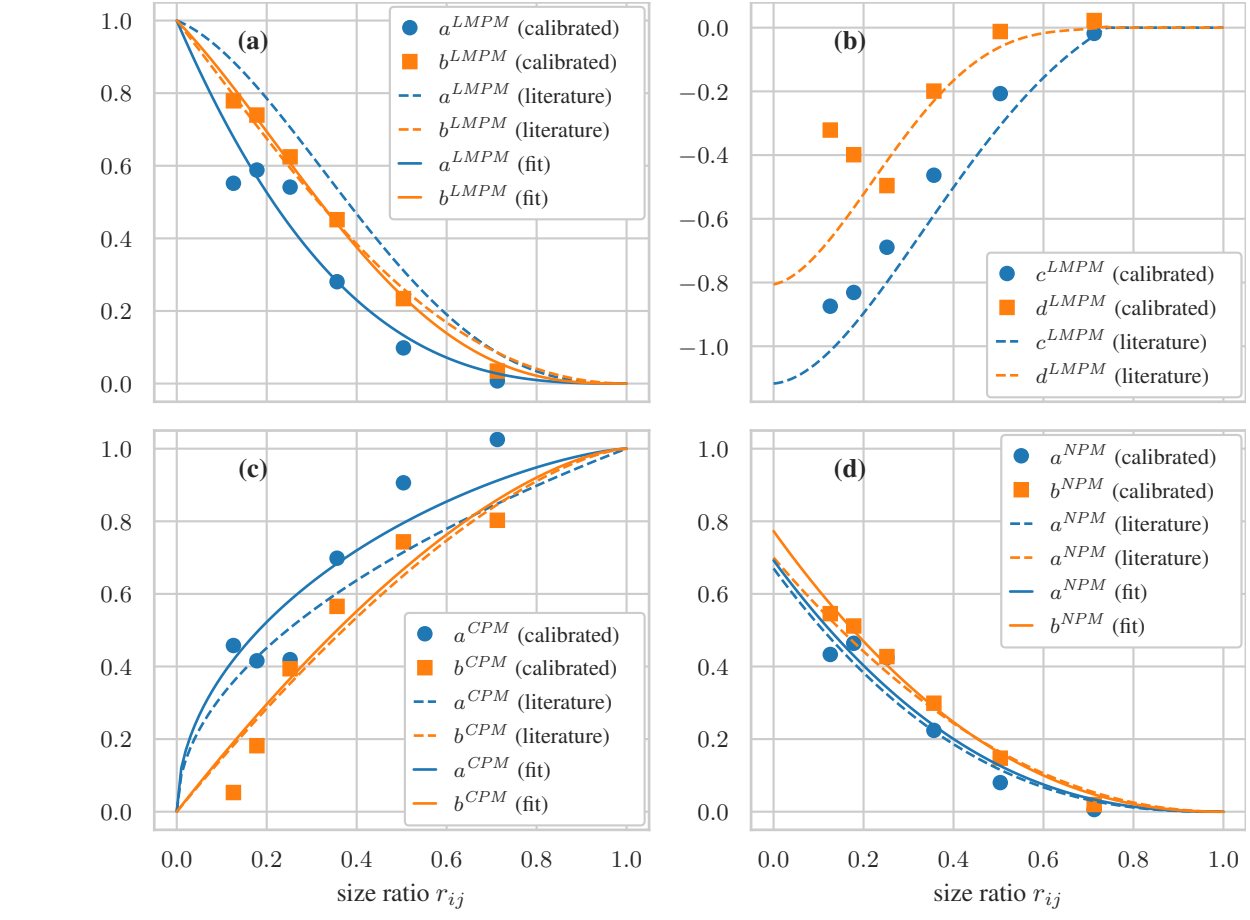

Figure 7. Interaction parameters of the different prediction models for the simulated binary setups with Rhine sediment. **a** LPM, **b** MM, **c** CPM, **d** NPM.

as suggested for vibrated packings (De Larrard, 1999). The result for the different models is shown in Fig. 6 where additionally the overall R^2 values and root mean square errors (RMSE) are given. All of those individually calibrated models were able to yield accurate predictions for the here considered binary cases, with slightly better results for CPM and NPM.

The obtained interaction parameters for each model are shown in Fig. 7 as a function of the size ratio alongside the interaction function, parameterized as proposed in literature (see Appendix A). While in some cases, e.g., NPM, a good agreement between both could be seen, larger deviations were generally observed, e.g., for LPM. These differences are expected as the majority of the suggested parameterizations were obtained for spherical particles whereas the interaction depends on the shape. Therefore, we fitted the individual interaction functions with the help of their coefficients to our obtained interaction parameters, as suggested by others (Kwan et al., 2015; Liu et al., 2019). The resulting fitted interaction functions are also shown in Fig. 7, and the corresponding coefficients are reported in Table 2. For LPM and NPM, the agreement between the individually obtained parameters and the fitted functions is overall very good. For the CPM, however, the functional form itself with only

https://doi.org/10.5194/esurf-2022-72
Preprint. Discussion started: 23 January 2023


Earth Surface Dynamics Discussions
Open Access
EGU

Table 2. Interaction function and fitted coefficients as shown in Fig. 7.

Model	Function	Parameters
LPM	Eq. (A3)	$A_1^{LMPM} = 2.899$, $A_2^{LMPM} = 0.026$, $A_3^{LMPM} = 2.725$
	Eq. (A4)	$B_1^{LMPM} = 3.033$, $B_2^{LMPM} = 1.762$, $B_3^{LMPM} = 2.866$
CPM	Eq. (A7)	$A_1^{CPM} = 1.429$
	Eq. (A8)	$B_1^{CPM} = 1.573$
NPM	Eq. (A9)	$A_1^{NPM} = 0.692$, $A_2^{NPM} = 2.428$
	Eq. (A10)	$B_1^{NPM} = 0.773$, $B_2^{NPM} = 2.234$

one coefficient seems to be insufficient to accurately capture the actual trend which would call for an in-depth investigation and improvement of the model for binary packings. For the MM, we refrained from fitting the interaction function since the proposed functions Eqs. (A5) and (A6) contain too many coefficients that would promote overfitting and the additional dependency on porosity would require much more data. Still, the original functions exhibited a reasonable agreement with the found parameters. Combining the findings for the individual model calibration and the fitting of the interaction functions, we find that the NPM works overall best for the case considered here.

This step finalized the calibration of the interaction functions for all models which we kept as here determined for the remainder of this work.

4 Validation against simulations

This section validates the packing models with the just calibrated interaction functions for continuous size distributions, containing coarse sand to gravel. The reference results were again obtained by means of numerical simulations.

4.1 Simulation setup

The packings were simulated and evaluated with the same method as for the binary packings in Sect. 3. This way, it is ensured that also all process-related factors that possibly influence the packing behavior are similar to the setup used for the calibration. This controlled environment thus effectively removes sources of uncertainties usually present in experiments and allows for a direct analysis of the packing models' predictive power.

Packing simulations become increasingly challenging for larger size differences as the number of particles grows cubically and numerical stability has to be ensured at the cost of smaller time steps. To limit the computational cost of the present simulations, we restricted this validation study to a narrow size range that corresponds to coarse sand and gravel. For the first set of setups, we applied the same seven size fractions as in Table 1. There, we used the six size distributions already considered by Liang et al. (2015) and Rettinger et al. (2022b), i.e., unimodal and bimodal distributions obtained from different log-normal distributions. Additionally, seven random size distributions for the same size range and for an extended size range, respectively,

https://doi.org/10.5194/esurf-2022-72
Preprint. Discussion started: 23 January 2023

were generated. The extended size range added two smaller sieve mesh sizes, 1.4 mm - 2 mm and 2 mm - 2.8 mm, to the ones given in Table 1, resulting in nine size classes. Generally, for N size fractions, these random size distributions were constructed by selecting $N-1$ random numbers, sampled from a uniform distribution between 0 and 1. Those numbers, together with the values 0 and 1, were then sorted in ascending order to yield the discretized cumulative distribution function, from which the mass fractions per size class could be obtained as the difference of neighboring values.

Thus, in total, 20 size distributions were simulated and we provide their size distributions and evaluated porosity values in the supplementary material.

4.2 Evaluation

To obtain the porosity prediction, the coefficients of all interaction functions were taken as found via the previous calibration study and given in Table 2. Additionally, and again as before, we set $n_{0,i} = 0.338$ as initial porosity for all size classes. Therefore, no anew adaption of the models to the validation data had been carried out here.

The evaluation of the obtained predictions for the three different models for the 20 size distributions is shown in Fig. 8, together with the R^2 score and the RMSE. There, the LMPM exhibited the overall best prediction performance, only slightly worse than for the bidisperse cases in Fig. 6. It was closely followed by the CPM with an error of 0.01. The NPM showed a systematic overprediction in porosity with maximum errors up to 0.046 and a large RMSE. This deviation is in stark contrast to its accurate predictions of the bidisperse case and might hint towards intrinsic deficits for such multi-sized packings.

These findings revealed that the NPM does not permit accurate porosity predictions for continuous size distributions, whereas this is seemingly the case for LMPM and CPM. One possibly decisive difference between these two groups is that the LMPM and CPM both have built-in mixture models for the size class i, either explicitly via the MM or implicitly via the compaction model. Such a model is absent in the NPM which, by construction, assumes that only a single size class i forms the dominant component, see Fig. 2. To partially check this assumption, we additionally used the LPM, i.e., the LMPM without mixture packing model, and the MM, i.e., the LMPM without linear packing model. The outcome is also shown in Fig. 8, in the second row. The predictions from the LPM visually exhibited a strong resemblance to the NPM with mostly too large predicted porosity values, especially for the intermediate value range, resulting in large errors. In contrast, the MM produced results that are almost identical to the LMPM, indicating that for the here considered, comparably narrow, grain size range such a mixture model is of vital importance as no single size class can really be considered dominant, as assumed in the NPM. Since adding a mixture model to the NPM is not straightforward, we decided to exclude this packing model from further comparisons.

5 Application and comparison to fluvial data

As a final step, we applied the prediction models to laboratory measurement data obtained for sediment from different rivers. This data contained samples in the size range of 0.02 mm to 200 mm, thus from silt to coarse gravel, which significantly extends the size range compared to the previous validation.

https://doi.org/10.5194/esurf-2022-72
Preprint. Discussion started: 23 January 2023

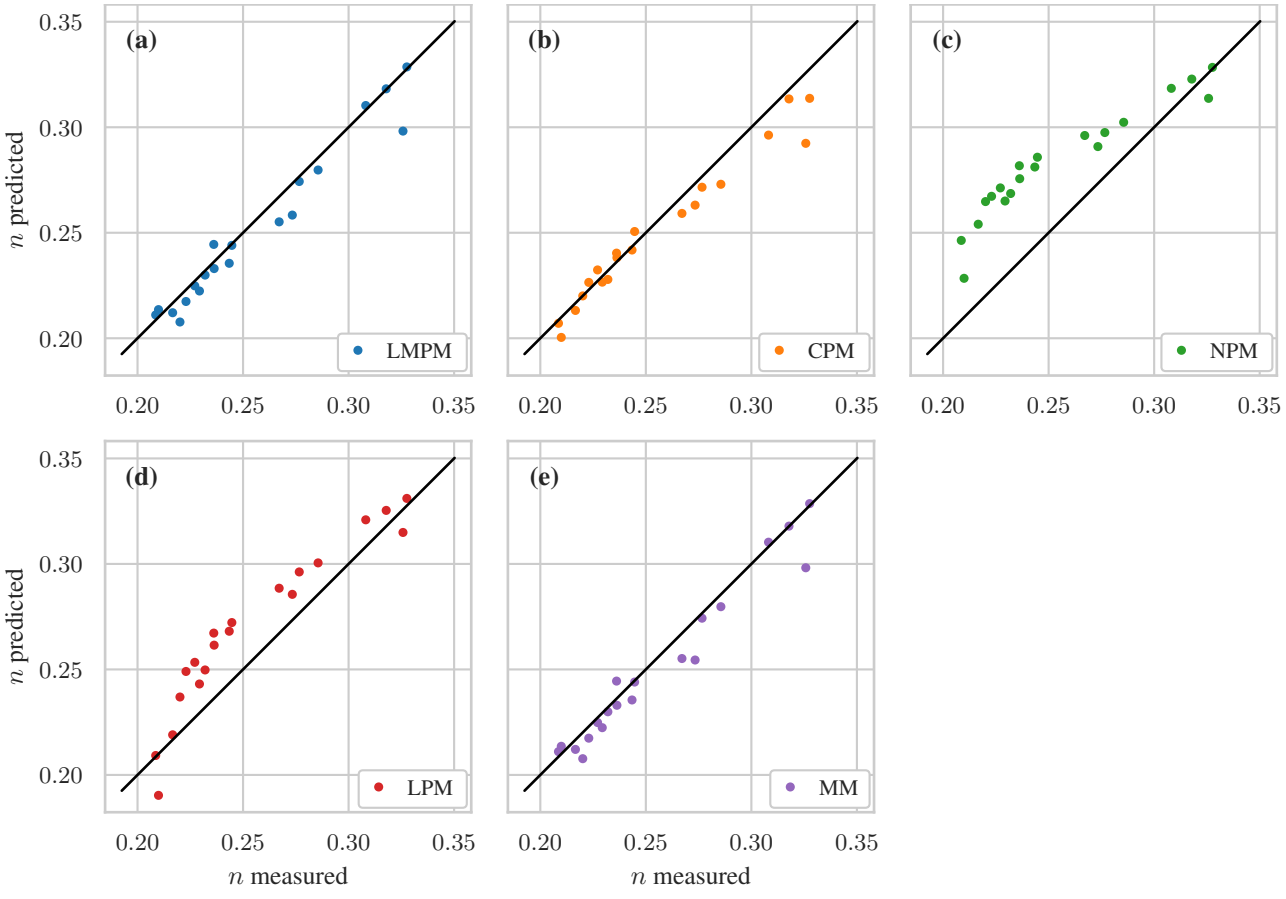

Figure 8. Measured (from simulations) vs. predicted porosity for the different packing models. **a** LMPM ($R^2 = 0.946$, RMSE $= 0.009$), **b** CPM ($R^2 = 0.931$, RMSE $= 0.010$), **c** NPM ($R^2 = 0.308$, RMSE $= 0.032$), **d** LPM ($R^2 = 0.762$, RMSE $= 0.019$), **e** MM ($R^2 = 0.942$, RMSE $= 0.009$).

5.1 Modeling the effect of cohesion

The packing of very fine particles, like clay or fine silt, differs from larger particles as additional particle interactions, like van der Waals or electrostatic forces, can become dominant over all other, friction-based or gravitational, forces. As a result, such particles often form aggregates (Yu et al., 2003; Zou et al., 2011). This cohesion effect strongly depends on actual particle size, here generally assumed to become notable when the grain size is below a critical value d_c^{coh}, and influences porosity. Consequently, in order to accurately describe packings that at least partially contain the particle sizes where such effects are relevant, cohesion has to be included in the prediction model. These cohesion models are briefly outlined next.

https://doi.org/10.5194/esurf-2022-72
Preprint. Discussion started: 23 January 2023

Earth Surface Dynamics Discussions
Open Access
EGU

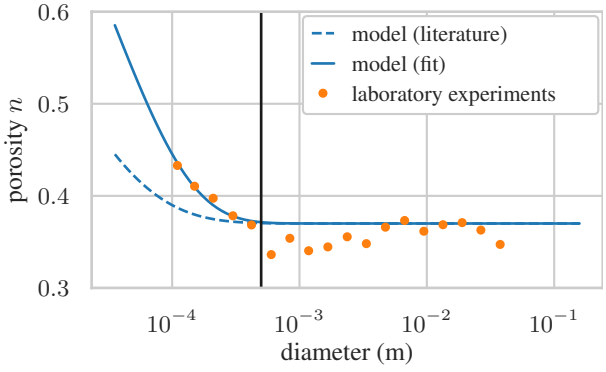

Figure 9. Effect of cohesion on porosity of uniform packings of a given mean diameter. Data from laboratory experiments with sediment from the Rhine River (Frings et al., 2011), corrected for edge effects of the used container for the measurements. The solid black vertical line denotes the assumed d_c^{coh}.

By considering uniform packings, Yu et al. (1997) modeled the increase of porosity due to cohesive interactions for small particle sizes by

$$\tilde{n}_{0,i} = n_{0,i} + (1 - n_{0,i}) \exp(-e^{coh} (d_i/d_{ref})^{f^{coh}}), \tag{19}$$

where we introduced $d_{ref} = 10^{-3}$ m, as also used to define the phi size scale, to remove the units from the original expression. The two coefficients e^{coh} and f^{coh} depend on particle shape and the packing process, and need to be calibrated to measurements (Yu et al., 1997). There, Yu et al. (2003) suggested $e^{coh} = 10.141$ and $f^{coh} = 0.468$ which was also adopted by Zou et al. (2011) and showed a good agreement for particles and powders used in industrial applications. Based on these findings, the critical grain size for cohesion was estimated to be around 0.15 mm for dry glass beads (Zou et al., 2011) and sand (El-Husseiny, 2020).

For fluvial sediment, we carried out an analogous evaluation to determine suitable coefficients of Eq. (19) and the critical cohesion size. This analysis is shown in Fig. 9 for the porosity values obtained by Frings et al. (2011) from laboratory measurements of uniform packings of sediment taken from the Rhine River. A strong increase in porosity for small particles is clearly visible for diameters smaller than roughly 0.5 mm, which we take as d_c^{coh}. Using the average porosity $n_{0,i} = 0.37$ reported for the laboratory measurements, we fitted Eq. (19) to the data and obtained $e^{coh} = 8.916$ and $f^{coh} = 0.615$. The resulting curve was able to predict the increase in porosity, improving upon the available parameterization.

In addition to affecting the porosity of uniform packings, Yu et al. (1997) noticed that the interaction among different size classes changes once cohesive effects play a role. As, e.g., small particles would not simply fill the void between larger particles but might form agglomorates or stick to the larger particles' surface, the gaps inside the packing are increased which, by implication, increases porosity. Thus, the binary interactions expressed by the size ratio r_{ij} and the interaction functions in the packing models should be adapted as well. For that reason, a modified size ratio was proposed (Zou et al., 2011), given as

$$\tilde{r}_{ij} = (1 - \xi^{coh}) (r_{ij})^{p^{coh}} + \xi^{coh} r_{ij}, \tag{20}$$

https://doi.org/10.5194/esurf-2022-72
Preprint. Discussion started: 23 January 2023


Earth Surface Dynamics Discussions Open Access EGU

where the coefficient $p^{coh} \in [0,1]$ quantifies the cohesive packing degree. The weighting factor ξ^{coh} combines the actual size ratio r_{ij} for coarse particles with a power-law model for the fine ones (Yu et al., 1997), and was determined as

$$\xi^{coh} = \begin{cases} 1, & d_i \geq d_c^{coh}, \\ 0, & d_j \leq d_c^{coh}, \\ 1 - 1.543 \exp(-0.697 d_j / d_c^{coh}), & d_i \leq d_c^{coh} \leq d_j, \end{cases} \tag{21}$$

for $d_i < d_j$ (Zou et al., 2011). For the coefficient p^{coh}, values of 0.15 for natural sand-silt mixtures (El-Husseiny, 2020) up to 0.593 for alumina powder (Yu et al., 1997) have been suggested and applied successfully. As the former is presumably similar to fluvial sediment, we adopted $p^{coh} = 0.15$, noting, however, that an appropriate choice might also depend on the packing conditions (Yu et al., 1997). Following these model assumptions, the interaction functions were here left unchanged and evaluated with the modified size ratio $\tilde{r}_{ij}$ instead of the nominal one.

5.2 Data from the Rhine River

As part of their porosity measurement campaign in the Rhine River, Frings et al. (2011) carried out 46 laboratory measurements with sediment obtained from sub-surface layers of the channel bed and river bank, consisting mainly of quartz. The sediment was put inside a cylindrical container and the water displacement method was used to determine porosity of the individual samples that featured a size range of 0.02 mm - 200 mm.

To set up the porosity predictors for this data set, we assumed that the sediment form was generally similar to the ones we used for calibration in Sect. 3. This can be justified as the samples for the CT scans were taken from the sediment used in the laboratory measurements, even though the calibration only made use of gravel-sized grains. Consequently, we applied the same interaction functions as in Sect. 4. The initial porosity $n_{0,i}$ was taken as 0.37 for all size classes, corresponding to the average of the laboratory measurements with uniform packings with similar sediment (Frings et al., 2011). This choice was made to rule out further factors possibly influencing porosity, like process-based ones, and put the predictions and the measurements on the same basis. Since the packings contained very fine grains below the assumed size threshold for cohesion, $d_c^{coh} = 0.5$ mm that we determined above, we used the adaptions as given by Eqs. (19) and (20) to incorporate the effect of cohesion by increasing the initial porosity of small size classes and redefining the size ratio. For comparison, we carried out predictions with the original and the cohesion-modified variant of the LMPM and the CPM.

The outcome of this comparative study is stated in Table 3 and visualized in Fig. 10. The original variants of LMPM and CPM did not perform well, with low determination coefficients and high mean and maximum errors. As can be seen, both models underpredicted porosity for almost all packings. Once the modifications by the cohesion model were included, the predictions improved significantly in both cases. There, the CPM was performing best and achieved a mean error of 0.038 while the LMPM still exhibited larger errors and a only a low R^2 score. This improvement was apparently achieved by an increase in the predicted porosity for all cases, which is in agreement with the expected action of cohesion in packings.

https://doi.org/10.5194/esurf-2022-72
Preprint. Discussion started: 23 January 2023

Earth Surface Dynamics Discussions
Open Access
EGU

Table 3. Comparison of porosity prediction performance (R^2, root-mean-square error RMSE, and maximum absolute error ME) of packing models for the Rhine River data (Frings et al., 2011).

	original			with cohesion model		
	R^2	RMSE	ME	R^2	RMSE	ME
LMPM	-0.023	0.068	0.180	0.384	0.053	0.094
CPM	0.356	0.054	0.187	0.689	0.038	0.096

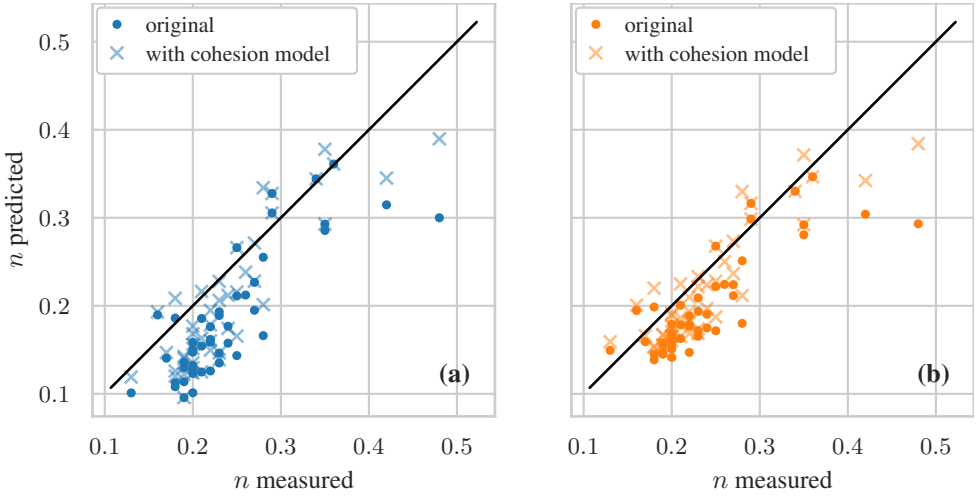

Figure 10. Measured (from laboratory) vs. predicted porosity for the different packing models with fluvial sediment from the Rhine River (Frings et al., 2011). **a** LMPM, **b** CPM.

5.3 Data from the Bès and Galabre River

To investigate the generalizability of the packing models and their parameterizations to other rivers, we made use of a second extensive data set obtained by Tabesh et al. (2022) from the banks of two rivers in the Rhône-Alpes in France, named Bès and Galabre. They are significantly smaller than the Rhine, and feature a different composition of the sediment, both in terms of lithology and shape. Samples were collected at four different sites with varying sediment characteristics, and their porosity was analyzed later in the laboratory via the water displacement method. The resulting 52 data points again featured size distributions in the range of 0.02 mm - 200 mm. In contrast to the Rhine data set above, no information about the porosity values of uniform packings of the different size classes was provided, and also no details about form characteristics of the sediment were given.

Therefore, in the context of the packing models, no calibration of the interaction and cohesion models was possible as in Sects. 3 and 5.1 for the Rhine River, and we kept the same parameterization as for the Rhine. Also, $n_{0,i}$ as one of the major input quantities of the models remained unknown. We varied its value in the interval $[0.37, 0.49]$ as a sensitivity study, always keeping it constant for all size classes but allowing for modifications based on the cohesion model via Eq. (19).

https://doi.org/10.5194/esurf-2022-72
Preprint. Discussion started: 23 January 2023

Earth Surface Dynamics Discussions
Open Access
EGU

Table 4. Comparison of porosity prediction performance (R^2 score, root-mean-square error RMSE, and maximum absolute error ME) of packing models for the data from the Bès and Galabre River (Tabesh et al., 2022), for varying values of the assumed initial porosity $n_{0,i}$. RMSE values given in bold indicate the best outcome for a certain model.

	$n_{0,i}$	0.37	0.39	0.41	0.43	0.45	0.47	0.49
LMPM + cohesion								
	R^2	-1.168	-0.611	-0.111	0.293	0.574	0.725	0.733
	RMSE	0.101	0.087	0.073	0.058	0.045	**0.036**	**0.036**
	ME	0.159	0.148	0.136	0.123	0.109	0.096	0.084
CPM ($K = 9$) + cohesion								
	R^2	-0.273	0.165	0.506	0.733	0.828	0.774	0.550
	RMSE	0.078	0.063	0.048	0.036	**0.029**	0.033	0.046
	ME	0.135	0.118	0.101	0.084	0.066	0.081	0.103
CPM ($K = 4$) + cohesion								
	R^2	0.557	0.724	0.777	0.706	0.496	0.135	-0.390
	RMSE	0.046	0.036	**0.032**	0.037	0.049	0.064	0.081
	ME	0.120	0.101	0.084	0.084	0.102	0.121	0.141

The results of this study are given in Table 4. The value of the initial porosity had a significant influence on the prediction quality. For the value of 0.37, that we used for the Rhine River and where it provided reasonable predictions for both packing models, none of the two was able to yield satisfactory results for the present data set, with mean errors of more than 0.078. The agreement improved for increasing initial porosity values, where a value of 0.45 was the most accurate choice for the CPM and 0.47 to 0.49 for the LMPM. Since both models consistently required such a large initial porosity, one could assume that its actual value might be in the same region. Such a large value would hint towards packing conditions that result in a rather loose packing state.

By construction, the CPM allows for another option to account for loose rather than dense packings, i.e., via the compaction index K. Using $K = 4$, as suggested for loose packing conditions, instead of $K = 9$ as for all previous results, the most accurate prediction was achieved with an initial porosity of 0.41. This difference is primarily achieved by the model-internal modification of the ideal packing densities via Eq. (15), which has a similar effect as providing a larger initial porosity value.

5.4 Discussion

Applying the packing models as porosity predictors to actual fluvial sediment data has revealed their capabilities but also some challenges. The latter primarily arose in the determination or estimation of the various input parameters and quantities, i.e., the initial porosity and the interaction functions that depend on the particle shape. To facilitate the following discussion, we provide a sketch of the different components of a packing model in Fig. 11.

https://doi.org/10.5194/esurf-2022-72
Preprint. Discussion started: 23 January 2023

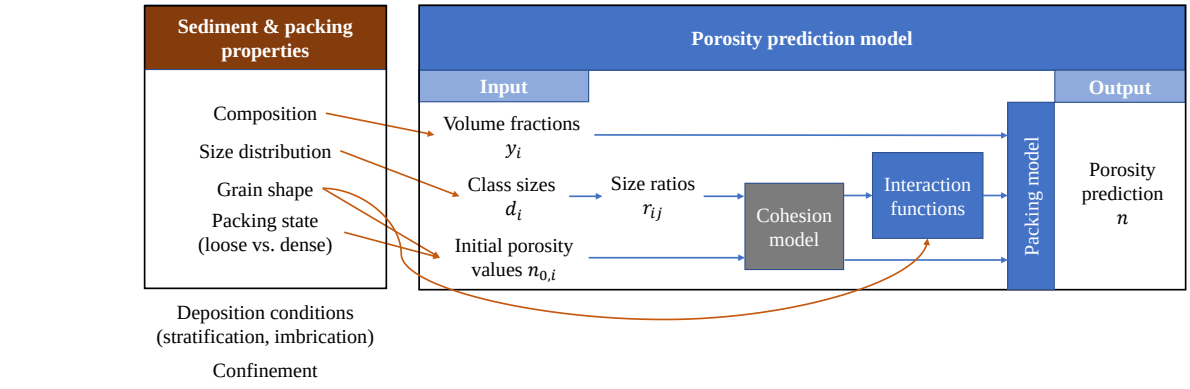

Figure 11. Sketch of the packing model and its parameterization. The brown arrows denote the influence of a property on one of the model components as considered in the present work. Blue arrows indicate the flow of data within the model.

Two of the main model parameters, the volume fractions y_i and corresponding size information d_i were here determined by sieving the collected samples in the laboratory, a standard procedure which is thus not considered problematic. If the sediment density is known to vary for the size classes, e.g., as a result of different lithologies in the deposit, these variations should be accounted for when converting the mass fractions to volume fractions. Especially for field studies, photogrammetric approaches are a promising alternative to sieving but are currently still limited to rather large grain sizes (Mair et al., 2022).

Regarding the other relevant parameters, the above study with the Rhine data can be considered as the ideal case. Since we had some digital scans of similar sedimentary grains available, simulations were used to calibrate the interaction functions to binary packings (cf. Sect. 3). The common alternative would be to carry out such measurements in a laboratory setting (Yu et al., 1996; De Larrard, 1999; Liu et al., 2019). The following validation in Sect. 4 with simulated packings under exactly equal conditions but various size distributions showcased that accurate predictions are possible with these packing models. When applied directly to laboratory measurements, however, differences already occurred in the initial porosity $n_{0,i}$. Here, it had to be adapted to the one found in laboratory which was larger (0.37) than the one found via simulations (0.338). Furthermore, these laboratory measurements of uniform packings were also useful to parameterize the cohesion model which turned out to be of importance for such wide size distributions containing very fine grains. The porosity predictions that we achieved by this combination of findings from laboratory measurements and simulation were reasonably accurate, given the fact that also other effects might perturb the measured data, like the porosity-increasing effect of the container boundaries and the top of the packing. Such influence factors were fully captured by the applied measurement method in the laboratory but were not accounted for by the packing model, and also excluded in the simulations.

For the comparison to the data from the two French rivers, neither detailed information about the sediment form nor dedicated measurements of uniform packings were available This lack of information made it necessary to assume that the Rhine-based parameterization of the interaction functions and the cohesion model were still applicable here. This might be justified since the actual sediment form is probably similar to the one of the Rhine sediment and thus no large deviation from the

https://doi.org/10.5194/esurf-2022-72
Preprint. Discussion started: 23 January 2023

calibrated parameters can be expected. A major challenge, however, was to determine the initial porosity for each size class. The subsequent sensitivity study revealed its large influence on the resulting predictions. In practice, the initial porosity that resulted in the best predictions for the available data could be used to essentially calibrate this input to the cases at hand, i.e., specific to the fluvial environment.

Generally, if form information like the average elongation or flatness is available, the porosity predictions for dense uniform packings derived by Rettinger et al. (2022b) could be used to determine $n_{0,i}$ where the effect of form is explicitly taken into account. Since porosity also strongly depends on the packing conditions, available relations for minimal and maximal porosity of dense and loose packings, respectively, can be used to define a valid range of initial porosity values. For clean sand, e.g., the relation

$$e_{max} = 1.53\, e_{min} + 0.072 \tag{22}$$

was found for the two limiting void ratios (Cubrinovski and Ishihara, 2002). Assuming that the porosity of the dense uniform packing is 0.37, as for the Rhine laboratory measurements, then a porosity of 0.49 would correspond to the loose packing state according to this relation. Thus, the found initial porosity of roughly 0.46 for the French river case could be considered reasonable, provided that also the grain form was similar. Other, refined relations are available using form and shape information (Chang et al., 2018; Maroof et al., 2022). Alternatively, the CPM offers the possibility to adapt the compaction index K to account for different packing conditions which can be utilized to avoid supplying unreasonably large initial porosity values for this model.

If the actual form is strongly different from the here considered grains, then porosity measurements for uniform and binary packings should be carried out to verify or recalibrate the parameters of the interaction functions. This analysis can be achieved either in the laboratory or via simulations (Liu et al., 2017). Ideally, and if relevant for the case at hand, those studies could be extended to very small particles to capture the regime of cohesive interactions in order to determine the parameters of the cohesion model as well.

Moving towards field measurements, the challenges associated with the determination of the input variables grow further. There, the underlying model assumption that the packing is a random particle mixture could be violated by selective deposition conditions, that might have led to imbrication or stratification inside the sediment bed. Additionally, it is usually not possible to obtain field measurements for uniform packings as those do not occur naturally. These effects lead to additional uncertainties in the obtained predictions and might essentially limit the applicability of the models considered here. Advanced simulation studies, that closely resemble the deposition conditions in actual rivers, could be used there as a promising yet demanding alternative to determine the required model input and promote further model improvements.

All in all, the intrinsic complexity of particle packings with the large number of influence factors directly carries over to corresponding prediction models where all of them should be considered, i.e., modeled. The more of these factors can be quantified or excluded, the better the expected outcome using the here considered prediction models.

https://doi.org/10.5194/esurf-2022-72
Preprint. Discussion started: 23 January 2023

6 Conclusions

In this paper, we have presented and discussed three different porosity prediction models for the packing of fluvial sediment, which is characterized by a wide range of size ratios and complex particle shapes. These packing models, named Linear Mixture Packing Model (LMPM), Compressible Packing Model (CPM), and Nonlinear Packing Model (NPM), partition the particles into distinct size classes, for which the respective average size, the mass fraction per class, and porosity of a single class packing have to be provided. By considering the interaction between the contained size classes, modeled via interaction parameters and depending on the classes' size ratio, they provide predictions of porosity.

These interaction parameters were calibrated via packing simulations of several binary cases using digital scans of actual sediment grains from the Rhine River in Germany. This study showed that all of these packing models are able to capture binary cases well if calibrated adequately, with a slightly better performance of the NPM. Based on the individually calibrated cases, the models' interaction parameters could be formulated as functions of the size ratio, making them applicable for the general, multi-sized case.

This applicability was verified by 20 further simulations, now featuring continuous size distributions between 1.4 mm and 31.5 mm. Keeping all other variables, like packing process and porosity evaluation, the same, the accurate prediction capabilities of the LMPM and the CPM for this case were established. On the other hand, the outcome of the NPM revealed a systematic deficit for these continuous size distributions which we could attribute to a missing built-in mixture packing model for the dominant size class, as opposed to the two other models.

Finally, we applied the LMPM and the CPM to two different data sets obtained from laboratory porosity measurements with sediment from the Rhine River and two French rivers. Both featured size distributions ranging from 0.02mm to 200 mm, thus covering the range from silt to coarse gravel. There, we could demonstrate that the packing models should be augmented with a dedicated cohesion model as it improved the predictions significantly. However, the models were less accurate than for the simulation data since not all effects of the laboratory experiments could be quantified and were thus not included in the models. The comparison for the French rivers acted primarily as a sensitivity study regarding unknown input variables for the packing models, as here neither information about the size classes' porosity nor the sediment shape was available. Given a sensible estimate of single class porosity values, we could obtain reasonable prediction results. Based on these findings, we discussed several ways a suitable porosity predictor can be obtained for fluvial sediment deposits, with the general recommendation to make use of the CPM due to its flexibility.

Overall, we could showcase the great potential that lies within these theoretical packing models given a detailed knowledge of the packing process and some sediment properties. The observed discrepancy for the case of laboratory measurements and the expected even larger challenge for field measurements highlight that many different aspects of such a packing play a role that might not yet be properly accounted for in the present models or the provided model input. Further improvements are expected once recent extensions of the LMPM and the CPM, that aim to cover additional interaction effects among the size classes, become available for multi-sized packings, in combination with the here found importance of a proper mixture packing

https://doi.org/10.5194/esurf-2022-72
Preprint. Discussion started: 23 January 2023

Earth Surface Dynamics Discussions
Open Access
EGU

model as well as a cohesion model. Simulations, augmented by cohesive effects and featuring different deposition conditions, can here help to identify, quantify, and model these effects systematically.

Code and data availability. The simulation software, including the numerical method and the setups, is publicly available via WALBERLA's main repository (https://walberla.net). The sediment geometries used in the simulative studies are available on Zenodo (Rettinger et al., 2022c). Additionally, a Python implementation of the packing models including examples can be found on Zenodo (Rettinger and Frings, 2022) alongside the results of the binary and multi-sized packings obtained by the simulations presented here.

Appendix A: Details of packing models

A1 Linear Mixture Packing Model

The range of size classes that define the mixture for a specific class i are given as

$$L = \begin{cases} 1, & d_i/r_c > d_1, \\ j, & d_{j-1} \geq d_i/r_c > d_j, \quad j = 2,3,\ldots,i. \end{cases} \tag{A1}$$

$$M = \begin{cases} j, & d_j \geq d_i\, r_c > d_{j+1}, \quad j = i, i+1, \ldots, N-1, \\ N, & d_N > d_i\, r_c. \end{cases} \tag{A2}$$

This definition uses the modification proposed by Frings et al. (2008), who also provided a detailed explanation of the model.

The interaction parameters a^{LMPM} and b^{LMPM} are functions of the size ratio and were proposed as

$$a^{LMPM}(r_{ij}) = (1 - r_{ij})^{A_1^{LMPM}} + A_2^{LMPM} r_{ij} (1 - r_{ij})^{A_3^{LMPM}}, \tag{A3}$$

$$b^{LMPM}(r_{ij}) = (1 - r_{ij})^{B_1^{LMPM}} + B_2^{LMPM} r_{ij} (1 - r_{ij})^{B_3^{LMPM}}. \tag{A4}$$

By considering binary packings of spherical particles, Yu et al. (1996) determined the coefficients as $A_1^{LMPM} = 3.3$, $A_2^{LMPM} = 2.8$, $A_3^{LMPM} = 2.7$, $B_1^{LMPM} = 2.0$, $B_2^{LMPM} = 0.4$, and $B_3^{LMPM} = 3.7$.

The quadratic and cubic mixture parameters c^{LMPM} and d^{LMPM}, respectively, were found to be a function of the size ratio r_{jk} and the initial mixture porosity $n_{0,mix}$, as obtained from the specific volume ν_0^{mix} (Yu and Standish, 1991):

$$c^{LMPM}(r_{jk}, n_{0,mix}) = \begin{cases} 10.288 \times 10^{-1.4566\, n_{0,mix}} (-1.0002 + 0.1126 r_{jk} + \\ \quad 5.8455 r_{jk}^2 - 7.9488 r_{jk}^3 + 3.1222 r_{jk}^4), & r_{jk} \leq 0.741, \\ 0, & r_{jk} > 0.741, \end{cases} \tag{A5}$$

$$d^{LMPM}(r_{jk}, n_{0,mix}) = \begin{cases} (-1.3092 + 15.039\, n_{0,mix} - 37.453\, n_{0,mix}^2 + 40.869\, n_{0,mix}^3 - 17.110\, n_{0,mix}^4) \\ \quad (-1.0029 + 0.3589 r_{jk} + 10.970 r_{jk}^2 - 22.197 r_{jk}^3 + 12.434 r_{jk}^4), & r_{jk} \leq 0.741, \\ 0, & r_{jk} > 0.741. \end{cases} \tag{A6}$$

https://doi.org/10.5194/esurf-2022-72
Preprint. Discussion started: 23 January 2023

Earth Surface Dynamics Discussions
Open Access
EGU

A2 Compressible Packing Model

The model's interaction parameters, a^{CPM} and b^{CPM}, are functions of the size ratio r_{ij} and were found from binary experiments with rounded and crushed aggregates as

$$a^{CPM}(r_{ij}) = \sqrt{1-(1-r_{ij})^{A_1^{CPM}}}, \tag{A7}$$

$$b^{CPM}(r_{ij}) = 1-(1-r_{ij})^{B_1^{CPM}}, \tag{A8}$$

with coefficients $A_1^{CPM} = 1.02$ and $B_1^{CPM} = 1.5$ (De Larrard, 1999).

A3 Nonlinear Packing Model

The two interaction functions, a^{NPM} and b^{NPM} are generally given as

$$a^{NPM}(r_{ij}) = A_1^{NPM}(1-r_{ij})^{A_2^{NPM}}, \tag{A9}$$

$$b^{NPM}(r_{ij}) = B_1^{NPM}(1-r_{ij})^{B_2^{NPM}}, \tag{A10}$$

where the coefficient values $A_1^{NPM} = 0.670$, $A_2^{NPM} = 2.508$, $B_1^{NPM} = 0.700$, and $B_2^{NPM} = 2.065$ were extracted from experiments with binary spherical glass beads (Liu et al., 2019).

Appendix B: Binary versions of packing models

In the following, we state the binary versions of the packing models presented in Sect. 2 which were then used in Sect. 3.

B1 Linear Mixture Packing Model

As the LMPM (Yu and Standish, 1991; Yu et al., 1996) combines a linear packing model and a mixture packing model with individual parameters we consider them separately here. The specific volume according to the linear packing model (LPM) for a binary packing is (Yu et al., 1996):

$$v = \max(\nu_1 y_1 + \nu_2(1-a_{12}^{LMPM})y_2, (\nu_1-(\nu_1-1)b_{21}^{LMPM})y_1 + \nu_2 y_2) \tag{B1}$$

with parameters a_{12}^{LMPM} and b_{21}^{LMPM}. The mixture packing model (MM) for a binary packing is given as

$$v = y_1\nu_1 + y_2\nu_2 + c_{12}^{LMPM} y_1 y_2 + d_{12}^{LMPM} y_1 y_2 (y_1 - y_2) \tag{B2}$$

with parameters c_{12}^{LMPM} and d_{12}^{LMPM}.

https://doi.org/10.5194/esurf-2022-72
Preprint. Discussion started: 23 January 2023

Earth Surface Dynamics Discussions
Open Access
EGU

B2 Compressible Packing Model

The packing densities of the two ideal packings considered by the CPM (De Larrard, 1999) are given as

$$\gamma_1 = \frac{\beta_1}{1-(1-a_{12}^{CPM}\frac{\beta_1}{\beta_2})y_2}, \tag{B3}$$

$$\gamma_2 = \frac{\beta_2}{1-(1-\beta_2+b_{21}^{CPM}\beta_2(1-\frac{1}{\beta_1}))y_1} \tag{B4}$$

with the parameters a_{12}^{CPM} and b_{21}^{CPM}. The final ϕ is obtained by solving the quadratic equation

$$K = \frac{y_1/\beta_1}{1/\phi - 1/\gamma_1} + \frac{y_2/\beta_2}{1/\phi - 1/\gamma_2} \tag{B5}$$

for the chosen value of K.

B3 Nonlinear Packing Model

The void ratio of a binary packing according to the NPM (Liu et al., 2019) is given as

$$e = \max\left(\epsilon_1 y_1^2 - \epsilon_2 y_2^2 + 2\epsilon_2 y_2 - a_{12}^{NPM}(\epsilon_2(1+y_1)+1)y_2, \epsilon_2 y_2^2 - \epsilon_1 y_1^2 + 2\epsilon_1 y_1 - b_{21}^{NPM}\epsilon_1(1+y_2)y_1\right) \tag{B6}$$

with the parameters a_{12}^{NPM} and b_{21}^{NPM}.

Author contributions. CR and RF conceptualized the study. CR performed the simulations, developed the model implementation, and carried out the analysis. MT and RF compiled and prepared the laboratory measurement data. CR prepared the manuscript with contributions from all co-authors. RF acquired the funding. UR provided access to the computational resources. SV administered the project.

Competing interests. The authors declare no competing interests.

Acknowledgements. The authors want to thank Axel Winterscheid and Wenjia Xu for fruitful discussions that helped to shape the research. CR gratefully acknowledges the support through the German Research Foundation (DFG) grant FR 3509/4-2, awarded to RF. UR is grateful for the support through the DFG project 433735254. The authors gratefully acknowledge the HPC resources provided by the Erlangen National High Performance Computing Center (NHR@FAU) of the Friedrich-Alexander-Universität Erlangen-Nürnberg (FAU). NHR funding is provided by federal and Bavarian state authorities. NHR@FAU hardware is partially funded by the DFG - 440719683. Furthermore, the authors gratefully acknowledge the Gauss Centre for Supercomputing e.V. (www.gauss-centre.eu) for funding this project by providing computing time on the GCS Supercomputer SuperMUC-NG at Leibniz Supercomputing Centre (www.lrz.de).

https://doi.org/10.5194/esurf-2022-72
Preprint. Discussion started: 23 January 2023

References

An, X. Z., Yang, R. Y., Zou, R. P., and Yu, A. B.: Effect of vibration condition and inter-particle frictions on the packing of uniform spheres, Powder Technology, 188, 102–109, https://doi.org/10.1016/j.powtec.2008.04.001, 2008.

Bauer, M., Eibl, S., Godenschwager, C., Kohl, N., Kuron, M., Rettinger, C., Schornbaum, F., Schwarzmeier, C., Thönnes, D., Köstler, H., and Rüde, U.: waLBerla: A block-structured high-performance framework for multiphysics simulations, Computers & Mathematics with Applications, 81, 478–501, https://doi.org/10.1016/j.camwa.2020.01.007, 2021.

Carling, P. A. and Reader, N. A.: Structure, composition and bulk properties of upland stream gravels, Earth Surface Processes and Landforms, 7, 349–365, https://doi.org/10.1002/esp.3290070407, 1982.

Chan, K. and Kwan, A.: Evaluation of particle packing models by comparing with published test results, Particuology, 16, 108–115, https://doi.org/10.1016/j.partic.2013.11.008, 2014.

Chang, C. S. and Deng, Y.: A particle packing model for sand–silt mixtures with the effect of dual-skeleton, Granular Matter, 19, 1–15, https://doi.org/10.1007/s10035-017-0762-1, 2017.

Chang, C. S. and Deng, Y.: A nonlinear packing model for multi-sized particle mixtures, Powder Technology, 336, 449–464, https://doi.org/10.1016/j.powtec.2018.06.008, 2018.

Chang, C. S., Deng, Y., and Meidani, M.: A multi-variable equation for relationship between limiting void ratios of uniform sands and morphological characteristics of their particles, Engineering Geology, 237, 21–31, https://doi.org/10.1016/j.enggeo.2018.02.003, 2018.

Cho, G.-C., Dodds, J., and Santamarina, J. C.: Particle Shape Effects on Packing Density, Stiffness, and Strength: Natural and Crushed Sands, Journal of Geotechnical and Geoenvironmental Engineering, 132, 591–602, https://doi.org/10.1061/(ASCE)1090-0241(2006)132:5(591), 2006.

Coleman, S. E. and Nikora, V. I.: Exner equation: A continuum approximation of a discrete granular system, Water Resources Research, 45, https://doi.org/10.1029/2008WR007604, 2009.

Cubrinovski, M. and Ishihara, K.: Maximum and Minimum Void Ratio Characteristics of Sands, Soils and Foundations, 42, 65–78, https://doi.org/doi.org/10.3208/sandf.42.6_65, 2002.

De Larrard, F.: Concrete mixture proportioning: a scientific approach, CRC Press, https://doi.org/10.1201/9781482272055, 1999.

El-Husseiny, A.: Improved Packing Model for Functionally Graded Sand-Fines Mixtures—Incorporation of Fines Cohesive Packing Behavior, Applied Sciences, 10, https://doi.org/10.3390/app10020562, 2020.

Fraser, H. J.: Experimental Study of the Porosity and Permeability of Clastic Sediments, The Journal of Geology, 43, 910–1010, https://doi.org/10.1086/624388, 1935.

Frings, R. M., Kleinhans, M. G., and Vollmer, S.: Discriminating between pore-filling load and bed-structure load: a new porosity-based method, exemplified for the river Rhine, Sedimentology, 55, 1571–1593, https://doi.org/10.1111/j.1365-3091.2008.00958.x, 2008.

Frings, R. M., Schüttrumpf, H., and Vollmer, S.: Verification of porosity predictors for fluvial sand-gravel deposits, Water Resources Research, 47, https://doi.org/10.1029/2010WR009690, 2011.

Furnas, C.: Grading aggregates-I.-Mathematical relations for beds of broken solids of maximum density, Industrial & Engineering Chemistry, 23, 1052–1058, https://doi.org/10.1021/ie50261a017, 1931.

Jones, M., Zheng, L., and Newlands, M.: Comparison of particle packing models for proportioning concrete constitutents for minimum voids ratio, Materials and structures, 35, 301–309, https://doi.org/10.1007/BF02482136, 2002.

https://doi.org/10.5194/esurf-2022-72
Preprint. Discussion started: 23 January 2023

Kamann, P. J., Ritzi, R. W., Dominic, D. F., and Conrad, C. M.: Porosity and Permeability in Sediment Mixtures, Groundwater, 45, 429–438, https://doi.org/10.1111/j.1745-6584.2007.00313.x, 2007.

Knop, Y. and Peled, A.: Packing density modeling of blended cement with limestone having different particle sizes, Construction and Building Materials, 102, 44–50, https://doi.org/10.1016/j.conbuildmat.2015.09.063, 2016.

Kwan, A., Chan, K., and Wong, V.: A 3-parameter particle packing model incorporating the wedging effect, Powder Technology, 237, 172–179, https://doi.org/10.1016/j.powtec.2013.01.043, 2013.

Kwan, A., Wong, V., and Fung, W.: A 3-parameter packing density model for angular rock aggregate particles, Powder Technology, 274, 154–162, https://doi.org/10.1016/j.powtec.2014.12.054, 2015.

Liang, R., Schruff, T., Jia, X., Schüttrumpf, H., and Frings, R. M.: Validation of a stochastic digital packing algorithm for porosity prediction in fluvial gravel deposits, Sedimentary Geology, 329, 18–27, https://doi.org/10.1016/j.sedgeo.2015.09.002, 2015.

Liu, Q., Jia, D., and Miao, J.: Study of the linear and nonlinear packing model based on mixing of quartz sand, Powder Technology, 366, 382–394, https://doi.org/10.1016/j.powtec.2020.02.056, 2020.

Liu, W., Chen, S., and Li, S.: Influence of adhesion on random loose packings of binary microparticle mixtures, AIChE Journal, 63, 4296–4306, https://doi.org/10.1002/aic.15775, 2017.

Liu, Z.-R., Ye, W.-M., Zhang, Z., Wang, Q., Chen, Y.-G., and Cui, Y.-J.: A nonlinear particle packing model for multi-sized granular soils, Construction and Building Materials, 221, 274–282, https://doi.org/10.1016/j.conbuildmat.2019.06.075, 2019.

Mair, D., Do Prado, A. H., Garefalakis, P., Lechmann, A., Whittaker, A., and Schlunegger, F.: Grain size of fluvial gravel bars from close-range UAV imagery – uncertainty in segmentation-based data, Earth Surface Dynamics, 10, 953–973, https://doi.org/10.5194/esurf-10-953-2022, 2022.

Maroof, M. A., Mahboubi, A., Vincens, E., and Noorzad, A.: Effects of particle morphology on the minimum and maximum void ratios of granular materials, Granular Matter, 24, 41, https://doi.org/10.1007/s10035-021-01189-0, 2022.

Noack, M., Ortlepp, J., and Wieprecht, S.: An Approach to Simulate Interstitial Habitat Conditions During the Incubation Phase of Gravel-Spawning Fish, River Research and Applications, 33, 192–201, https://doi.org/10.1002/rra.3012, 2017.

Oakey, R. J., Green, M., Carling, P. A., Lee, M. W., Sear, D. A., and Warburton, J.: Grain-shape analysis—A new method for determining representative particle shapes for populations of natural grains, Journal of Sedimentary Research, 75, 1065–1073, https://doi.org/10.2110/jsr.2005.079, 2005.

Perera, C., Wu, W., and Knack, I.: Porosity of bimodal and trimodal sediment mixtures, International Journal of Sediment Research, 37, 258–271, https://doi.org/10.1016/j.ijsrc.2021.09.008, 2022.

Rettinger, C. and Frings, R. M.: Packing Models for Porosity Prediction, Zenodo, https://doi.org/10.5281/zenodo.7465313, 2022.

Rettinger, C., Eibl, S., Rüde, U., and Vowinckel, B.: Rheology of mobile sediment beds in laminar shear flow: effects of creep and polydispersity, Journal of Fluid Mechanics, 932, A1, https://doi.org/10.1017/jfm.2021.870, 2022a.

Rettinger, C., Rüde, U., Vollmer, S., and Frings, R. M.: Effect of sediment form and form distribution on porosity: a simulation study based on the discrete element method, Granular Matter, 24, https://doi.org/10.1007/s10035-022-01275-x, 2022b.

Rettinger, C., Rüde, U., Vollmer, S., and Frings, R. M.: Effect of Sediment Form and Form Distribution on Porosity, Zenodo, https://doi.org/10.5281/zenodo.6412071, 2022c.

Roquier, G.: The 4-parameter Compressible Packing Model (CPM) for crushed aggregate particles, Powder Technology, 320, 133–142, https://doi.org/10.1016/j.powtec.2017.07.028, 2017.

https://doi.org/10.5194/esurf-2022-72
Preprint. Discussion started: 23 January 2023

Schruff, T., Liang, R., Rüde, U., Schüttrumpf, H., and Frings, R.: Generation of dense granular deposits for porosity analysis: assessment and application of large-scale non-smooth granular dynamics, Computational Particle Mechanics, 5, 59–70, https://doi.org/10.1007/s40571-016-0153-0, 2018.

Seelen, L. J. H., Padding, J. T., and Kuipers, J. A. M.: A granular Discrete Element Method for arbitrary convex particle shapes: Method and packing generation, Chemical Engineering Science, 189, 84–101, https://doi.org/10.1016/j.ces.2018.05.034, 2018.

Seitz, L., Haas, C., Noack, M., and Wieprecht, S.: From picture to porosity of river bed material using Structure-from-Motion with Multi-View-Stereo, Geomorphology, 306, 80–89, https://doi.org/10.1016/j.geomorph.2018.01.014, 2018.

Suhr, B. and Six, K.: Simple particle shapes for DEM simulations of railway ballast: influence of shape descriptors on packing behaviour, Granular matter, 22, 1–17, https://doi.org/10.1007/s10035-020-1009-0, 2020.

Tabesh, M., Hoffmann, T., Vollmer, S., Schüttrumpf, H., and Frings, R. M.: In-situ measurement of river-bed sediment porosity using Structure-from-Motion image analysis, Geomorphology, 338, 61–67, https://doi.org/10.1016/j.geomorph.2019.04.011, 2019.

Tabesh, M., Vollmer, S., Schüttrumpf, H., and Frings, R. M.: Spatial variability in river bed porosity determined by nuclear density gauging: A case study from a French gravel-bed river, Sedimentology, 69, 823–844, https://doi.org/10.1111/sed.12928, 2022.

Westman, A. E. R.: The packing of particles: empirical equations for intermediate diameter ratios, Journal of the American Ceramic Society, 19, 127–129, https://doi.org/10.1111/j.1151-2916.1936.tb19809.x, 1936.

Wooster, J. K., Dusterhoff, S. R., Cui, Y., Sklar, L. S., Dietrich, W. E., and Malko, M.: Sediment supply and relative size distribution effects on fine sediment infiltration into immobile gravels, Water Resources Research, 44, https://doi.org/10.1029/2006WR005815, 2008.

Wu, W. and Li, W.: Porosity of bimodal sediment mixture with particle filling, International Journal of Sediment Research, 32, 253–259, https://doi.org/10.1016/j.ijsrc.2017.03.005, 2017.

Wu, W. and Wang, S. S. Y.: Formulas for Sediment Porosity and Settling Velocity, Journal of Hydraulic Engineering, 132, 858–862, https://doi.org/10.1061/(ASCE)0733-9429(2006)132:8(858), 2006.

Yu, A. B. and Standish, N.: Estimation of the porosity of particle mixtures by a linear-mixture packing model, Industrial & engineering chemistry research, 30, 1372–1385, https://doi.org/10.1021/ie00054a045, 1991.

Yu, A. B., Zou, R. P., and Standish, N.: Modifying the Linear Packing Model for Predicting the Porosity of Nonspherical Particle Mixtures, Industrial & Engineering Chemistry Research, 35, 3730–3741, https://doi.org/10.1021/ie950616a, 1996.

Yu, A. B., Bridgwater, J., and Burbidge, A.: On the modelling of the packing of fine particles, Powder Technology, 92, 185–194, https://doi.org/10.1016/S0032-5910(97)03219-1, 1997.

Yu, A. B., Feng, C. L., Zou, R. P., and Yang, R. Y.: On the relationship between porosity and interparticle forces, Powder Technology, 130, 70–76, https://doi.org/10.1016/S0032-5910(02)00228-0, 2003.

Zhang, T., Zhang, C., Yang, Q., and Fu, R.: Inter-particle friction and particle sphericity effects on isotropic compression behavior in real-shaped sand assemblies, Computers and Geotechnics, 126, 103 741, https://doi.org/10.1016/j.compgeo.2020.103741, 2020.

Zhang, Z. F., Ward, A. L., and Keller, J. M.: Determining the Porosity and Saturated Hydraulic Conductivity of Binary Mixtures, Vadose Zone Journal, 10, 313–321, https://doi.org/10.2136/vzj2009.0138, 2011.

Zhao, S., Zhang, N., Zhou, X., and Zhang, L.: Particle shape effects on fabric of granular random packing, Powder Technology, 310, 175–186, https://doi.org/10.1016/j.powtec.2016.12.094, 2017.

Zou, R. P. and Yu, A. B.: The packing of spheres in a cylindrical container: the thickness effect, Chemical Engineering Science, 50, 1504–1507, https://doi.org/10.1016/0009-2509(94)00483-8, 1995.

https://doi.org/10.5194/esurf-2022-72
Preprint. Discussion started: 23 January 2023

Zou, R. P., Gan, M. L., and Yu, A. B.: Prediction of the porosity of multi-component mixtures of cohesive and non-cohesive particles, Chemical Engineering Science, 66, 4711–4721, https://doi.org/10.1016/j.ces.2011.06.037, 2011.